Synthesis, electrochemistry, UV/VIS/NIR spectroelectrochemistry and ZINDO calculations of a dinuclear ruthenium complex of the tetraoxolene bridging ligand 9-phenyl-2,3,7-trihydroxy-6-fluorone

Anita M. Barthram and Michael D. Ward*

School of Chemistry, University of Bristol, Cantock's Close, Bristol, UK BS8 1TS.
E-mail: mike.ward@bristol.ac.uk

Received (in Cambridge, UK) 29th March 2000, Accepted 11th May 2000
Published on the Web 14th June 2000

Reaction of 9-phenyl-2,3,7-trihydroxy-6-fluorone (H_3L) with $[Ru(bipy)_2(H_2O)_2]^{2+}$ affords the complex $[\{Ru(bipy)_2\}_2(\mu\text{-}L)]^+$ (**3**$^+$) which was isolated as its hexafluorophosphate salt; in this complex a $\{Ru(bipy)_2\}^{2+}$ fragment is coordinated to each dioxolene-like terminus of the bridging ligand $[L]^{3-}$. Voltammetric experiments in MeCN show the presence of three reversible one-electron redox couples at -0.36, 0.00 and $+0.53$ V *vs.* ferrocene/ferrocenium, which means that the complex is part of a four-membered redox chain spanning the oxidation states **3**$^+$ to **3**$^{4+}$. A spectroelectrochemical study in MeCN at $-30\,^{\circ}C$ reveals a complicated series of electronic spectra in the different oxidation states which include some intense transitions in the near-IR region of the spectrum. The spectra could be partly assigned with the assistance of ZINDO calculations, which show that extensive mixing between the metal-centred and bridging-ligand-centred orbitals occurs; metal-to-ligand charge-transfer, ligand-to-ligand charge-transfer and intra-ligand transitions, amongst others, could be identified.

Complexes of the chelating dioxolene ligand series ([catecholate]$^{2-}$, [semiquinonate]$^-$ and quinone; hereafter abbreviated as cat, sq and q, respectively) have been studied extensively because of their electrochemical and spectroscopic behaviour.[1–3] A major focus of this interest is in the internal charge distribution of the complexes, because extensive mixing of metal-based and ligand-based orbitals means that oxidation state assigments for metal and ligand are not always clear and 'redox isomerism' can even occur as two forms interchange.[4,5]

Lever *et al.* have shown that in the $[Ru(bipy)_2(OO)]^{n+}$ series [where 'OO' denotes a dioxolene ligand without specifying oxidation state; $n = 0$, 1, 2] the ruthenium centre is in the $+2$ oxidation state throughout, with the different oxidation states arising from ligand-based redox processes between the catecholate, semiquinonate and quinone forms.[6] In the Ru(II)–semiquinone and Ru(II)–quinone forms the complexes display intense, low-energy Ru(II) → OO MLCT transitions.[6] We have been interested in linking several of these $[Ru(bipy)_2(OO)]^{n+}$ units together by use of suitable bridging ligands which contain two or more dioxolene binding sites linked together.[7–10] The resultant complexes display a large number of well-separated redox processes largely centred on the bridging ligand, whose spectroelectrochemical properties are exceptionally rich. For example complex **1** (Fig. 1) undergoes four reversible one-electron interconversions linking five redox states in which the bridging ligand changes in steps from the fully reduced bis-catecholate to the fully oxidised bis-quinone; in this case the 'bis-semiquinone' state (as shown in Fig. 1) is diamagnetic due to formation of a double bond between the 'semiquinone' units and adoption of a planar, quinonoidal structure.[8] Likewise the trinuclear complex **2** can exist in seven redox states from the tris-catecholate to the tris-quinone.[10] The very strong MLCT transitions in the near-IR region displayed by these complexes in some oxidation states but not others makes them of potential interest as dyes for electro-optic switching in the near-IR region of the spectrum.[11–13]

We have extended our investigations to complexes with related bridging ligands based on two dioxolene sites, and describe here the preparation, electrochemical and spectroscopic properties of $[\{Ru(bipy)_2\}_2L]^{n+}$ ($n = 1$–4), where H_3L is 9-phenyl-2,3,7-trihydroxy-6-fluorone. Despite its obvious appeal as a bis-bidentate bridging ligand there is only a single

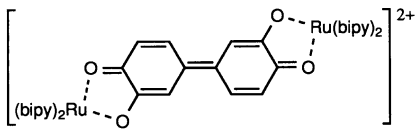

[**1**]$^{2+}$

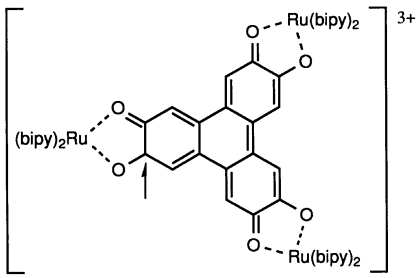

[**2**]$^{3+}$

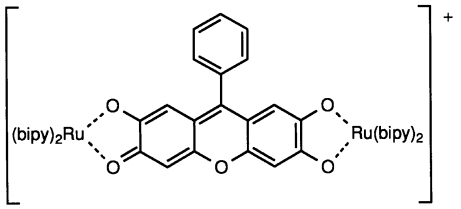

[**3**]$^+$

Fig. 1 Structures of complexes **1–3**. Complexes **1** and **2** are drawn with each dioxolene fragment in the semiquinone oxidation level, which is how the complexes are isolated; complex **3** is drawn in the fully reduced state (as isolated).

report of its use this way, in a dinuclear complex of Ni(II).[14] Although it has two dioxolene-like termini, the single carbon atom spacer linking the two rings suggest that the behaviour of this complex will be fundamentally different from that of **1** and **2**, but will have more in common with a recently-reported bis-catecholate ligand in which a methine unit links the two binding sites.[15,16]

Experimental

General details

Instrumentation used for routine spectroscopic and electrochemical measurements, and for low-temperature UV/VIS/NIR spectroelectrochemical studies, has been described earlier.[17] H_3L was obtained commercially (Aldrich) and used as received; $[Ru(bipy)_2Cl_2]\cdot 2H_2O$ was prepared according to the published method.[18] ZINDO calculations were performed on a CAChe workstation.[19]

Synthesis of $[\{Ru(bipy)_2\}_2L][PF_6]$ [3(PF_6)]

To a suspension of $[Ru(bipy)_2Cl_2]\cdot 2H_2O$ (0.500 g, 0.96 mmol) in aqueous ethanol (50 cm^3, 1 : 1) was added $AgNO_3$ (0.347 g, 2.04 mmol) and the mixture was heated to reflux for 30 min to give a red solution containing $[Ru(bipy)_2(H_2O)_2]^{2+}$. This was filtered to remove the AgCl. H_3L (0.152 g, 0.48 mmol) and KOH (0.10 g, excess) were then added and the mixture was heated to reflux for a further 2 h. After removal of the EtOH under reduced pressure, addition of aqueous NH_4PF_6 precipitated the complex as a dark blue powder; this was filtered off and dried. Final purification by column chromatography on alumina using MeCN : toluene (3 : 2, v/v) as eluent gave the product as a blue-black solid in 60% yield. ES-MS: *m/z* 1290 (M^+), 1145 $(M - PF_6)^+$, 572 $(M - PF_6)^{2+}$.

Recrystallisation for elemental analysis produced a material whose analysis was consistent with aerial oxidation to give $[\mathbf{3}^{2+}(PF_6)_2]$, in agreement with its electrochemical behaviour (see Results and discussion). Found: C, 50.0; H, 2.6; N, 7.8. Required for $C_{59}H_{41}F_{12}N_8O_5P_2Ru_2$: C, 49.4; H, 2.9; N, 7.8%.

Results and discussion

Synthesis and electrochemical properties of 3(PF_6)

The complex **3**(PF_6), which is an intense blue-black colour, was simply prepared by reaction of the H_3L with two equivalents of $[Ru(bipy)_2(H_2O)_2]^{2+}$ under basic conditions, followed by treatment with NH_4PF_6 and chromatographic purification. The ^1H NMR spectrum contains numerous overlapping peaks in the aromatic region of the spectrum, but it is clear from the number of environments that the complex has twofold symmetry such that the two metal termini are equivalent. Despite the apparent asymmetry of the coordinated ligand it is easy to see how delocalistion renders the two sites equivalent (Fig. 2). The fact that the complex is diamagnetic confirms that it is in the fully reduced form with the bridging ligand carrying a 3− charge.

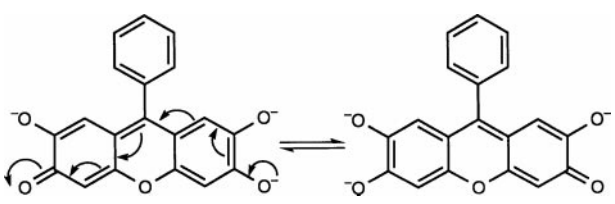

Fig. 2 Delocalisation in $[L]^{3-}$ which renders the two chelating sites equivalent.

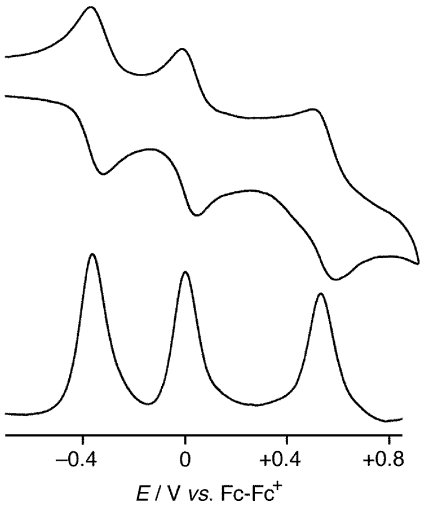

Fig. 3 Cyclic and square-wave voltammograms of $\mathbf{3}^+$ in MeCN, containing 0.1 M Bu_4NPF_6 as base electrolyte, using a Pt-bead working electrode and a scan rate of 0.1 V s^{-1}.

Cyclic and square-wave voltammetry of **3**(PF_6) in MeCN (Fig. 3) reveals three reversible, one-electron ($\Delta E_p = 60$–70 mV) processes at $E_{1/2} = -0.36$, 0.00 and +0.53 V *vs.* the ferrocene/ferrocenium couple (Fc/Fc^+). In addition there is a completely irreversible oxidation (no return wave) at +1.30 V *vs.* Fc/Fc^+, and some overlapping poorly-resolved irreversible reductions at potentials more negative than −2 V *vs.* Fc/Fc^+. By analogy with the properties of related Ru(II)/dioxolene/bipyridyl complexes such as dinuclear **1** and mononuclear $[Ru(bipy)_2(OO)]^{n+}$,[6,8] it is likely that: (i) some or all of the three reversible redox processes are centred on the bridging ligand; (ii) the irreversible wave at high positive potential is a metal-centred Ru(II)/Ru(III) process; and (iii) the irreversible waves at high negative potential are reductions of the terminal bipyridyl ligands. We note that the complex $[\{Ni(CTH)\}_2(\mu\text{-}L)]^+$ (CTH = 5,7,7,12,14,14-hexamethyl-1,4,8,11-tetraazacyclotetradecane) shows only two redox couples in this region, at −0.38 and +0.40 V *vs.* Fc/Fc^+, of which only the first was fully reversible and was assigned to a redox-centred L^{3-}/L^{2-} couple.[14] The presence of three redox processes in the same range for **3**(PF_6) suggests that at least one of them is formally metal-centred.

Whereas $\mathbf{3}^+$ is diamagnetic, the first oxidation product $\mathbf{3}^{2+}$ (formed by treatment of $\mathbf{3}^+$ with ferrocenium hexafluorophosphate) is paramagnetic, giving a broad EPR spectrum at 100 K (frozen CH_2Cl_2/thf glass) which shows an inflection at $g = 1.99$ with an additional feature on the low-field side at $g = 2.10$ (Fig. 4). As 0.5 and then 1.0 equivalents of ferrocenium hexafluorophosphate were added to the sample this signal grew in intensity; addition of excess ferrocenium hexafluorophosphate resulted in the signal diminishing in

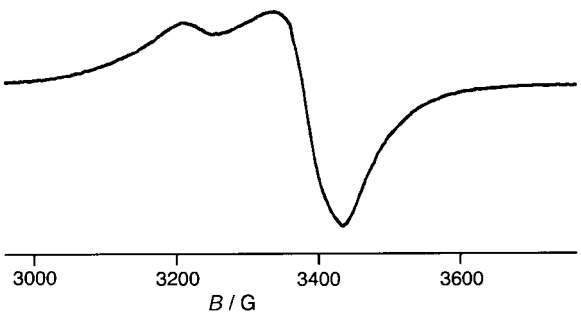

Fig. 4 EPR spectrum of $\mathbf{3}^{2+}$ (generated by oxidation of $\mathbf{3}^+$ with ferrocenium hexafluorophosphate) at 100 K in a CH_2Cl_2/thf glass.

intensity. This indicates that the doubly-oxidised complex $\mathbf{3}^{3+}$ starts to form and is diamagnetic.

Spectroelectrochemical study on 3(PF_6)

We have performed a UV/VIS/NIR spectroelectrochemical study on $\mathbf{3}^{+}$, spanning the four oxidation levels $\mathbf{3}^{+}$ (fully reduced, the form in which the complex is isolated) to $\mathbf{3}^{4+}$ for the dinuclear complex core, in MeCN at −30 °C; the results are shown in Fig. 5 and Table 1. All processes were found to be fully reversible, as shown by (i) the presence of clean isosbestic points for the overlaid spectra recorded during each redox conversion, and (ii) the complete regeneration of the spectrum of the starting material by re-reduction back to $\mathbf{3}^{+}$ at the end of the experiment.

For $\mathbf{3}^{+}$, apart from the usual $\pi \rightarrow \pi^*$ transitions of the bipy ligands in the UV region, the most prominent feature of the spectrum is an intense transition at 714 nm ($\varepsilon = 55\,000$ dm^3 mol^{-1} cm^{-1}). The ZINDO molecular orbital calculation on $\mathbf{3}^{+}$ showed that the HOMO (−8.03 eV) contains substantial contributions from both Ru atoms [20% total, using orbitals of d(π) symmetry] and the four terminal oxygen atoms of the bridging ligand [30% total, using orbitals of p(π) symmetry] with the remainder being delocalised over the skeleton of the bridging ligand. Just below this in energy (−8.6 to −9 eV) lie a closely-spaced set of similar orbitals which likewise contain contributions from both metals and bridging ligand. This suggests that the d(π) orbitals on each metal and the highest-energy filled orbitals of the bridging ligand have strongly mixed to the extent that a localised description of the orbitals as metal-centred or ligand-centred is unsatisfactory. Both the LUMO of $\mathbf{3}^{+}$ (−2.57 eV), as well as LUMO + 1 (−2.50 eV) are simply bipy-centred π* orbitals, as expected; however at about the same energy is the lowest π* level of the bridging ligand L^{3-} (LUMO + 2, −2.40 eV).

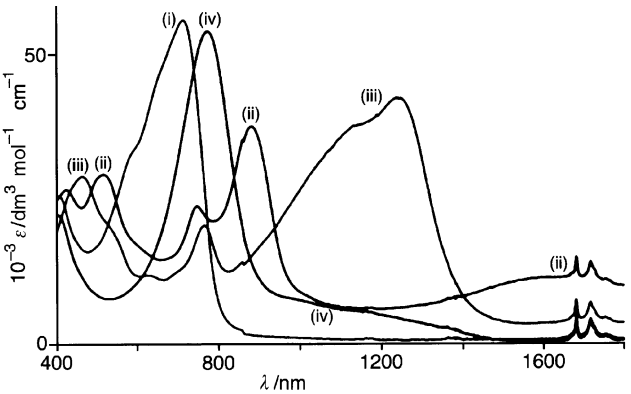

Fig. 5 Electronic spectra of (i) $\mathbf{3}^{+}$, (ii) $\mathbf{3}^{2+}$, (iii) $\mathbf{3}^{3+}$ and (iv) $\mathbf{3}^{4+}$ from the spectroelectrochemical experiment (MeCN, −30 °C).

Table 1 Electronic spectra of complex **3** in its different oxidation states (MeCN, −30 °C)

Complex	λ_{max}/nm ($10^{-3}\varepsilon$/dm^3 mol^{-1} cm^{-1})
$\mathbf{3}^{+}$	714(55), 582(sh), 407(23), 354(24), 294(120), 245(99)
$\mathbf{3}^{2+}$	1655(12), 882(36), 748(21), 517(24), 427(24), 292(150), 245(99)
$\mathbf{3}^{3+}$	1237(41), 1137(sh), 765(18), 545(sh), 465(26), 346(sh), 290(130), 244(100)
$\mathbf{3}^{4+}$	1100(sh), 775(54), 406(20), 285(87), 246(84)

Simulation of the electronic spectrum using the ZINDO method showed that the broad transition at 714 nm (predicted $\lambda_{max} = 445$ nm, predicted $\varepsilon = 109\,000$ dm^3 mol^{-1} cm^{-1})† contains at least 10 closely-spaced components involving all of these orbitals [HOMO → LUMO, HOMO − 1 → LUMO; HOMO → LUMO + 1; HOMO → LUMO + 2 *etc.*] [see Fig. 6(a)]. The HOMO → LUMO and related transitions are therefore charge-transfer in origin, from a delocalised metal/bridging ligand orbital to the bipyridyl π* levels. In simple terms these are analogous to the near-overlapping Ru[d(π)] → bipy MLCT and catecholate → bipy LLCT transitions of mononuclear [Ru(bipy)$_2$(cat)] which occur at *ca.* 620 and 725 nm respectively.[8] In addition, transitions such as HOMO → LUMO + 2, involving the lowest π* level of the bridging ligand L, have a combination of Ru → L MLCT and intra-ligand $\pi \rightarrow \pi^*$ characters. In agreement with this, the spectroscopically simpler complex [{Ni(CTH)}$_2$(μ-L)]$^+$ has a strong transition at 588 nm which was assigned as a $\pi \rightarrow \pi^*$ transition of the bridging ligand, and such a transition is one component of this manifold for **3**(PF_6).

On oxidation to $\mathbf{3}^{2+}$, there are two significant changes: the transition at 714 nm in $\mathbf{3}^{+}$ is shifted to lower energy (882 nm, with a shoulder at 748 nm), and a new transition appears at *ca.* 1650 nm ($\varepsilon = 12\,000$ dm^3 mol^{-1} cm^{-1}). If we try to explain the behaviour in simple terms by analogy with the model compound series [Ru(bipy)(OO)]$^{n+}$, we expect that a formally ligand-centred oxidation will result in a low-lying SOMO just above the metal-centred d(π) levels {*cf.* oxidation of [Ru(bipy)$_2$(cat)] to [Ru(bipy)$_2$(sq)]$^+$}, resulting in a low-energy Ru → sq MLCT transition which occurs at 880 nm in [Ru(bipy)$_2$(sq)]$^+$.[6,8] On this basis we could reasonably assign the 882 nm transition of $\mathbf{3}^{2+}$ to an MLCT transition from Ru to the bridging ligand SOMO, subject to the caveats outlined

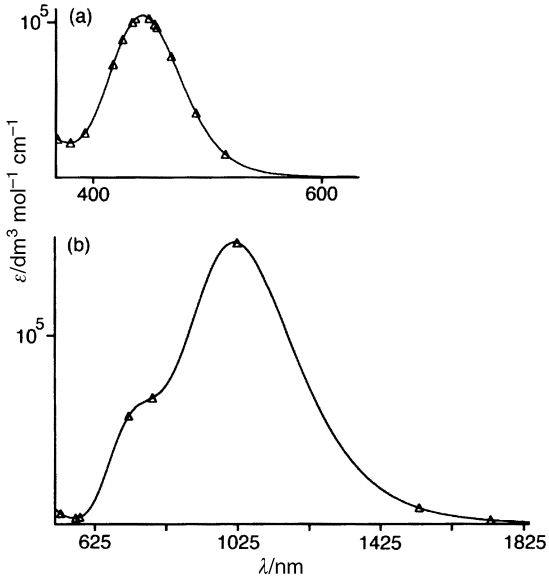

Fig. 6 Predicted electronic spectra (using the ZINDO method) of the diamagnetic complexes (a) $\mathbf{3}^{+}$ and (b) $\mathbf{3}^{3+}$, showing the positions of the individual components of each absorption envelope.

† The electronic spectral maxima as predicted by the ZINDO method for this series of complexes are consistently too high in energy (*e.g.* for $\mathbf{3}^{+}$, the 714 nm transition is predicted at 445 nm; for $\mathbf{3}^{3+}$, the 1237 nm transition is predicted at 1010 nm). However the numbers, relative energy ordering and approximate intensities of the transitions are consistent with what was observed, and the ZINDO calculations therefore give a reasonable *qualitative* picture of the behaviour of the complexes.

above regarding the limited accuracy of this localised description. The higher-energy transitions will include the Ru[d(π)] → bipy MLCT transitions which are still expected.

There are various possibilities for the broad near-IR transition at *ca.* 1650 nm. Its position and intensity are consistent with an inter-valence charge-transfer, either (i) from Ru(II) to Ru(III) following a metal-centred oxidation,[20] or (ii) from an electron-rich to an electron-poor end of the bridging ligand following a ligand-centred oxidation which is localised at one end.[21,22] In addition the spectrum of $[\{Ni(CTH)\}_2(\mu\text{-}L)]^{2+}$, in which the bridging ligand has been oxidised to $(L^{2-})^{\cdot}$, shows a transition at 1660 nm ($\varepsilon \approx 3000$ dm^3 mol^{-1} cm^{-1}) which was assigned to an intra-ligand transition involving the SOMO. It is likely that the true situation is a combination of these, with the low-energy transition being an 'end-to-end' charge-transfer from the non-oxidised Ru/dioxolene fragment to the oxidised one; it will therefore have both intra-ligand and charge-transfer character.

Further oxidation to $\mathbf{3}^{3+}$ results in the further red-shift of the "Ru(II) → L" MLCT transition to 1237 nm ($\varepsilon = 41\,000$ dm^3 mol^{-1} cm^{-1}), and the reduction in intensity of the weaker transition at 1650 nm that was apparent for $\mathbf{3}^{2+}$. Since this oxidation state is diamagnetic we could again carry out a ZINDO calculation to determine the molecular orbitals and help assign the electronic spectrum. The intense 1237 nm transition (predicted $\lambda_{max} = 1010$ nm; predicted $\varepsilon = 140\,000$ dm^3 mol^{-1} cm^{-1})† is the HOMO (−11.70 eV) → LUMO (−8.83 eV) transition, and we can draw an analogy with the mononuclear complex $[Ru(bipy)_2(q)]^{2+}$ in which there is a Ru → q MLCT transition into the low-lying orbital of the quinone which is now empty following two ligand-centred oxidations.[6] However examination of the form of the HOMO and LUMO of $\mathbf{3}^{3+}$ shows that this transition has very little MLCT character, as these frontier orbitals contain comparable contributions from metal and bridging ligand. The principal contributions to the HOMO are 36% from the Ru d(π) orbitals, with the remaining 64% evenly distibuted across the bridging ligand; for the LUMO the relative contributions are 25% from the metals and 75% from the bridging ligand. Thus the HOMO → LUMO transition has only slight MLCT character; it is more accurately a π → π* transition between two 'metal + bridging ligand' delocalised orbitals. We note also the presence of residual absorbance at around 1650 nm in the spectrum of $\mathbf{3}^{3+}$ which is not accounted for by the ZINDO calculation [Fig. 6(b)]; the cause of this is not clear at the moment.

Finally, oxidation to $\mathbf{3}^{4+}$ results in replacement of the 1237 nm transition of $\mathbf{3}^{3+}$ by one at much higher energy, at 775 nm ($\varepsilon = 54\,000$ dm^3 mol^{-1} cm^{-1}) with a low-energy shoulder at *ca.* 1100 nm. Assuming that the electron is removed from the HOMO of $\mathbf{3}^{3+}$ this is a highly delocalised transition which cannot be simply described as metal- or ligand-centred. By analogy with the spectrum of $\mathbf{3}^{2+}$ we assume that the relatively weak, lowest-energy transition at 1100 nm involves the singly-occupied orbital, and that the much more intense transition at 775 nm is a charge-transfer transition of some sort.

Conclusion

The new complex $\mathbf{3}^{+}$ has rich electrochemical behaviour, being the first member of a four-membered redox series which spans $\mathbf{3}^{+}$ to $\mathbf{3}^{4+}$. A UV/VIS/NIR spectroelectrochemical study showed the presence of intense transitions in the visible and near-IR region of the spectrum in all four oxidation states. These could be assigned to a limited extent with the help of ZINDO calculations on the complex in its diamagnetic oxidation states, which indicated that strong mixing between metal and ligand-centred orbitals results in delocalisation of the frontier orbitals, such that simple assignment of individual redox processes as metal- or ligand-based is not appropriate. The intense transitions in the near-IR region, and their strong variation with oxidation state over a four-membered redox series, make this compound of interest as an electrochromic near-IR dye.[10–13]

Acknowledgements

We thank the EPSRC for a project studentship (A.M.B.).

References

1 C. G. Pierpont and C. W. Lange, *Prog. Inorg. Chem.*, 1994, **41**, 331.
2 A. B. P. Lever, H. Masui, R. A. Metcalfe, D. J. Stufkens, E. S. Dodsworth and P. R. Auburn, *Coord. Chem. Rev.*, 1993, **125**, 317.
3 S. I. Gorelsky, E. S. Dodsworth, A. B. P. Lever and A. A. Vlcek, *Coord. Chem. Rev.*, 1998, **174**, 469.
4 A. S. Attia and C. G. Pierpont, *Inorg. Chem.*, 1998, **37**, 3051.
5 O. S. Jung, D. H. Jo, Y. A. Lee, B. J. Conklin and C. G. Pierpont, *Inorg. Chem.*, 1997, **36**, 19.
6 M. Haga, E. S. Dodsworth and A. B. P. Lever, *Inorg. Chem.*, 1986, **25**, 447.
7 M. D. Ward, *Inorg. Chem.*, 1996, **35**, 1712.
8 L. F. Joulié, E. Schatz, M. D. Ward, F. Weber and L. J. Yellowlees, *J. Chem. Soc., Dalton Trans.*, 1994, 799.
9 A. M. Barthram, R. L. Cleary, J. C. Jeffery, S. M. Couchman and M. D. Ward, *Inorg. Chim. Acta*, 1998, **267**, 1.
10 A. M. Barthram, R. L. Cleary, R. Kowallick and M. D. Ward, *Chem. Commun.*, 1998, 2695.
11 J. Fabian, H. Nakazumi and M. Matsuoka, *Chem. Rev.*, 1992, **92**, 1197.
12 (*a*) R. J. Mortimer, *Chem. Soc. Rev.*, 1997, **26**, 147; (*b*) R. J. Mortimer, *Electrochim. Acta*, 1999, **44**, 2971.
13 N. C. Harden, E. R. Humphrey, J. C. Jeffery, S.-M. Lee, M. Marcaccio, J. A. McCleverty, L. H. Rees and M. D. Ward, *J. Chem. Soc., Dalton Trans.*, 1999, 2417.
14 A. Dei, D. Gatteschi and L. Pardi, *Inorg. Chim. Acta*, 1991, **189**, 125.
15 D. A. Shultz, S. H. Bodnar, R. K. Kumar and J. W. Kampf, *J. Am. Chem. Soc.*, 1999, **121**, 10664.
16 D. A. Shultz and S. H. Bodnar, *Inorg. Chem.*, 1999, **38**, 591.
17 S.-M. Lee, R. Kowallick, M. Marcaccio, J. A. McCleverty and M. D Ward, *J. Chem. Soc., Dalton Trans.*, 1998, 3443.
18 B. P. Sullivan, D. J. Salmon and T. J. Meyer, *Inorg. Chem.*, 1978, **17**, 3334.
19 ZINDO version 4.0.2 in the CAChe system, Oxford Molecular, Oxford, 1998.
20 M. D. Ward, *Chem. Soc. Rev.*, 1995, 121.
21 N. C. Fletcher, T. C. Robinson, A. Behrendt, J. C. Jeffery, Z. R. Reeves and M. D. Ward, *J. Chem. Soc., Dalton Trans.*, 1999, 2999.
22 P. R. Auburn and A. B. P. Lever, *Inorg. Chem.*, 1990, **29**, 2551.